ACS POLYMERS Au
AN OPEN ACCESS JOURNAL OF THE AMERICAN CHEMICAL SOCIETY

pubs.acs.org/polymerau

Article

Unexpected Slow Relaxation Dynamics in Pure Ring Polymers Arise from Intermolecular Interactions

Michael Q. Tu, Oleg Davydovich, Baicheng Mei, Piyush K. Singh, Gary S. Grest, Kenneth S. Schweizer, Thomas C. O'Connor,* and Charles M. Schroeder*

Cite This: *ACS Polym. Au* 2023, 3, 307−317

Read Online

ACCESS | Metrics & More | Article Recommendations | Supporting Information

ABSTRACT: Ring polymers have fascinated scientists for decades, but experimental progress has been challenging due to the presence of linear chain contaminants that fundamentally alter dynamics. In this work, we report the unexpected slow stress relaxation behavior of concentrated ring polymers that arises due to ring−ring interactions and ring packing structure. Topologically pure, high molecular weight ring polymers are prepared without linear chain contaminants using cyclic poly(phthalaldehyde) (cPPA), a metastable polymer chemistry that rapidly depolymerizes from free ends at ambient temperatures. Linear viscoelastic measurements of highly concentrated cPPA show slow, non-power-law stress relaxation dynamics despite the lack of linear chain contaminants. Experiments are complemented by molecular dynamics (MD) simulations of unprecedentedly high molecular weight rings, which clearly show non-power-law stress relaxation in good agreement with experiments. MD simulations reveal substantial ring−ring interpenetrations upon increasing ring molecular weight or local backbone stiffness, despite the global collapsed nature of single ring conformation. A recently proposed microscopic theory for unconcatenated rings provides a qualitative physical mechanism associated with the emergence of strong inter-ring caging which slows down center-of-mass diffusion and long wavelength intramolecular relaxation modes originating from ring−ring interpenetrations, governed by the onset variable N/N_D, where the crossover degree of polymerization N_D is qualitatively predicted by theory. Our work overcomes challenges in achieving ring polymer purity and by characterizing dynamics for high molecular weight ring polymers. Overall, these results provide a new understanding of ring polymer physics.

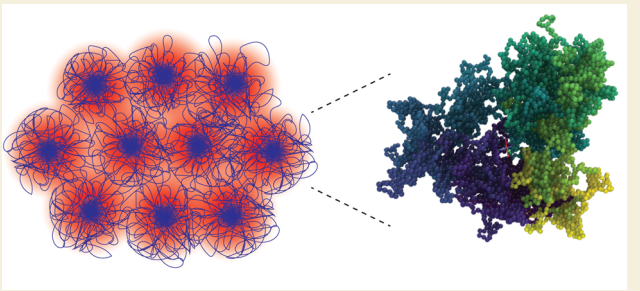

KEYWORDS: *ring polymers, polymer physics, stress relaxation, intermolecular correlations, glassy dynamics*

INTRODUCTION

Nearly all polymer architectures (e.g., linear, comb, star, bottlebrush) have free ends that play a key role in determining dynamics.[1−4] In concentrated solutions and melts, linear polymers relax stress by reptation,[1,5] where the dynamics are driven by polymer chain diffusion along the curvilinear backbone from a free end.[1] On the other hand, ring polymers are macromolecules with a circular topology lacking free ends.[6] Ring polymers are commonly found in biological systems, including circular prokaryotic genomes and plasmid-based DNA vaccines.[7−9] Polymer chemists recently synthesized interlocked rings based on poly[*n*]catenanes,[10] which provides access to new polymeric materials with distinct mechanical properties.[11] Due to the lack of free ends, ring polymers cannot relax stress by reptation, which necessitates a fundamentally different theoretical framework for understanding ring polymer dynamics.[12−15] Ring polymers are globally compact globules in concentrated solutions and melts, with a radius of gyration $R_g \sim N^{1/3}$, where N is the degree of polymerization.[16,17] Nevertheless, ring polymers are highly porous structures that exhibit large conformational fluctuations, giving rise to ring−ring interpenetrations or "threadings" in the condensed state.[16,18] Despite recent progress, understanding the role of inter-ring interpenetrations on stress relaxation dynamics remains an unsolved problem for mobile ring polymer liquids.

Experimental progress on ring polymer dynamics has been hindered due to challenges in both the synthesis and characterization of ring polymers. In recent years, single molecule experiments have been used to study the solution-phase dynamics of rings using DNA as a model polymer.[19] In dilute solutions, ring polymers unexpectedly undergo a shifted coil−stretch transition in planar extensional flow due to intramolecular hydrodynamic interactions,[20,21] and rings exhibit distinct conformational distributions in steady shear flow compared to linear chains.[22] In semidilute solutions of

Received: December 12, 2022
Revised: February 28, 2023
Accepted: March 1, 2023
Published: March 30, 2023

ring-linear blends, ring polymers exhibit multiple molecular subpopulations in relaxation and large conformational fluctuations in flow due to intermolecular interactions.[23−25] In the melt state, bulk rheology has been extensively used to characterize the dynamics of synthetic ring polymer melts, but experimental challenges arise due to the presence of linear chain contaminants generated as a byproduct of synthesis from ring-closure reactions.[26] Pioneering work on ring polystyrene melts revealed a reduced zero-shear viscosity for rings compared to linear polymers.[27] Following these early studies, new separation techniques based on liquid chromatography at the critical condition (LCCC) were used to improve the purity of ring polymer samples.[28] However, LCCC requires cumbersome preparation methods that hinder scale-up and unavoidably gives rise to samples with linear chain contaminants.[26,29] Tremendous effort has been directed at purifying ring polymer samples,[30−32] because even trace amounts of linear contaminants have been reported to significantly alter the rheological response of ring polymer melts.[26,33,34] Despite these challenges, LCCC-purified ring polymer samples were shown to exhibit power-law stress relaxation behavior,[33] which is fundamentally different than entangled linear polymer melts which show a rubbery plateau in stress relaxation.

Prior experiments on LCCC-purified polystyrene and polyisoprene ring polymer melts reported a power-law stress relaxation modulus $G(t) \propto t^{-\beta}$ in the intermediate time regime, where $0.4 \leq \beta \leq 0.5$,[33−35] which is consistent with weak or no deviations from the behavior of unentangled low molecular weight linear chains. However, prior work on polystyrene rings only focused on modest ring molecular weights, such that $N/N_e \lesssim 15$, where N_e is the number of monomers between entanglements for the equivalent linear chain chemistry.[33−35] Results from molecular dynamics (MD) simulations of highly flexible ring polymer melts with a broader range of degrees of entanglements ($N/N_e \lesssim 50$) are consistent with experimental results that also show a power-law stress relaxation.[17] Power-law exponents from experiments and MD simulations at these values of N/N_e generally agree with theoretical predictions from the fractal loopy globule (FLG) model with full dynamic dilution (or tube dilation),[13] which predicts $\beta = 3/7 \approx 0.43$. In addition, other theoretical models such as the double folded lattice animal (DFLA) model,[33] the annealed lattice animal model,[36] the so-called naive FLG model (which does not self-consistently account for tube dilation),[13] and the phenomenological free volume topological cage model[37] similarly provide reasonable agreement with prior reports of experimentally observed $G(t)$ behavior for ring polymer melts. Moreover, the models in these prior references[12,36,37] predict slightly delayed relaxation compared to the FLG model, i.e., smaller absolute values of the $G(t)$ power-law exponent as a function of time such that $G(t) \propto t^{-\beta}$, where $\beta = 0.40$ for the DFLA model, $\beta = 0.39$ for the annealed lattice animal model, and $\beta = 0.38$ for the naive FLG model.[13] However, none of these models predicts a fundamental deviation from the universal power-law stress relaxation behavior for ring polymer melts.

The FLG model describes ring dynamics in a melt as a series of self-similar loops rearranging on a time scale dictated by the loop size. The FLG model assumes $G(t)$ is governed by intraring dynamics and implicitly accounts for inter-ring interactions in a phenomenological manner through tube dilation.[13,14] Moreover, the FLG model postulates that entangled rings experience a dynamic dilution due to other rings relaxing. These scaling arguments predict a self-similar power-law stress relaxation with a constant exponent that is independent of N. Non-Fickian center-of-mass (COM) motion is not treated in the FLG theory, though it is essential for capturing caging effects in dense polymeric liquids.[15] When present, caging creates a localization length-scale that breaks dynamic self-similarity and can produce additional modes of intermolecular stress storage. Thus, the predictions of the FLG model are expected to break down if intermolecular interactions produce substantial caging of ring COM motion.[15,38] Interestingly, the FLG model predicts that stress relaxes faster in the terminal regime than observed in experiments based on ring polystyrene melts.[26] For example, prior work from Watanabe and co-workers on LCCC-purified rings found a different functional form of the time dependence of the long-time decay of $G(t)$ that is much slower than the decay predicted by the DFLA and FLG models.[26] This behavior calls into question whether LCCC-purified ring melts contain residual linear contaminants or if ring−ring interactions play a role in long-time stress relaxation in ring polymer melts.[33]

Molecular simulations show that entangled rings substantially interpenetrate, forming ring−ring threadings.[39−42] Some simulations show that ring−ring threadings can massively slow center-of-mass diffusion for semiflexible rings in concentrated solutions, albeit based on a model where a fraction of rings are artificially immobilized or pinned.[39,40] Based on an empirical extrapolation of results from the pinned ring simulations to the nonpinned mobile liquid limit of experimental interest, these simulations of semiflexible rings suggest that above a critical molecular weight, a kinetically arrested state emerges where individual polymers are caged and long-range motion is effectively frozen out on a practical simulation time scale.[39,40]

In terms of analytical modeling, a microscopic theory was recently developed that explicitly relates ring COM motion and dynamic caging to the time correlations of the intermolecular excluded volume forces between segments on different rings.[15,38] In this way, the microscopic theory is fundamentally different than the self-consistent FLG model[13] and the alternative models discussed above,[12,36,37] even in the "weak caging" regime where deviations from Rouse dynamics first emerge. None of these prior models[12,13,36,37] work at the level of time-correlations of molecular forces, as discussed at length in a recent publication.[15] Further descriptive review of the published Mei-Dell-Schweizer theory is provided later in this article. In brief, the theory predicts multiple regimes in ring diffusion, from Rouse-like to weak caging to a strong caging activated hopping regime, with increasing N, polymer concentration, and/or backbone stiffness. The theory was further shown to agree with results from MD simulations of flexible ring melts for the long time diffusion constant and subdiffusive COM dynamics on intermediate time scales.[15,17,38,43,44] We also note the recent experimental observation of anomalous COM subdiffusion in ring melts of modest molecular weight,[45] which was suggested to be related to the correlation hole effect, consistent with the qualitative spirit of the recent theoretical work.[15]

In order to understand the dynamics of topologically pure ring samples, we believe that an alternative theory is required that accounts for both intra- and inter-ring interactions. Such a framework would capture dynamical caging effects for high molecular weight rings, a regime that has been challenging to access in prior experiments and simulations of flexible ring

https://doi.org/10.1021/acspolymersau.2c00069
ACS Polym. Au 2023, 3, 307−317

polymer chemistries. Although prior simulation work on semiflexible rings reported a topological glass transition,[39,40] this phenomenon required the pinning or artificial localization of ring polymers on the computer. It is not known whether these transient localization effects emerge naturally in high molecular weight concentrated rings, which would allow access to the strong caging regime in real materials.

New polymer chemistries are required to enhance the purity of high molecular weight ring polymers for physical and rheological characterization. To this end, low-ceiling temperature polymer chemistry can be used to prepare rings free of linear chain contaminants. Polyphthalaldehyde (PPA) is a low ceiling temperature polymer (T_c = −36 °C)[46] that was developed for triggered degradation applications.[47−49] End-capped linear PPA has been shown to be thermally stable at temperatures up to 150 °C.[50] Without end-caps, PPA rapidly depolymerizes from free ends for temperatures $T > T_c$. Moore and co-workers discovered that cationic polymerization of *o*-phthalaldehyde monomers results in cyclic polymers[51] (Figure 1). In contrast to prior synthetic strategies for rings relying on

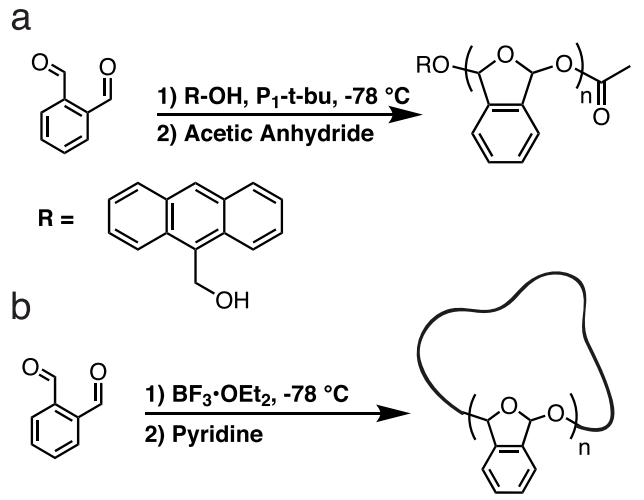

Figure 1. Reaction schemes for low-ceiling temperature polymer chemistry used in this work. (a) Anionic and (b) cationic polymerization schemes for poly(phthalaldehyde) (PPA) resulting in linear and ring topologies, respectively.

ring-closure reactions[52−54] or polymer-supporting reagents,[55] the cationic polymerization of phthalaldehyde is straightforward and readily amenable to large-scale, multigram syntheses without the need for tedious chromatographic purification to separate rings from linear chains. Synthesis of cyclic poly(phthalaldehyde) (cPPA) results in stable kinetically trapped ring polymers at ambient temperatures, as any linear PPA present during synthesis rapidly degrades when processed at elevated temperatures above approximately −40 °C. Moreover, if cPPA rings are unexpectedly cleaved during processing or rheological characterization, the linear chain product rapidly decomposes to monomer rather than remaining as linear chain contaminants.[26] Based on these triggered degradation properties, cPPA has recently been used to develop new transient materials[56,57] and fully recyclable plastics.[58]

In this work, we leverage the low-ceiling temperature properties of cPPA to study the rheology of pure ring polymers with extremely high molecular weights (Table 1). Linear viscoelastic measurements are performed on highly concentrated cPPA samples, and the stress relaxation response

Table 1. Properties of Synthesized Phthalaldehyde Polymers Used in This Work with Number of Entanglements per Equivalent Linear Chain $Z = M_w/M_e$ (SI)[a]

label	M_n (kDa)	M_w (kDa)	PDI	Z
L-180	172	182	1.06	10
R-80	51	76	1.50	4.3
R-150	98	154	1.57	8.6
R-500	316	473	1.50	26
R-1000	790	1050	1.33	59

[a]Absolute molecular weights are determined via GPC-MALS (Figure S2). Polymer topologies are denoted via L- and R- prefixes for linear and ring topologies, respectively.

is compared to results from MD simulations of ring polymers with unprecedented molecular weights. We use a combination of experiments and simulations to show that the intermediate stress relaxation response qualitatively differs from the predicted constant power-law behavior of FLG theory and shows a stress relaxation response very similar in shape to linear entangled polymers of the same chemistry. Our simulation results show that polymer backbone stiffness strongly affects ring polymer relaxation behavior, with stiffer backbone rings exhibiting slow relaxation dynamics at lower molecular weights than flexible rings due to enhanced inter-ring interactions. A recently proposed microscopic force level theory for unconcatenated polymer melts predicts the onset of a slowing down in COM diffusion and the terminal relaxation time,[15,38] which is attributed to intermolecular ring−ring interactions. We further show that the slowing-down of ring polymer dynamics depends systematically on polymer molecular weight and backbone stiffness, with the latter having a significant impact on ring relaxation dynamics. Overall, our results show that ring−ring interpenetration gives rise to new physics in the dynamics of densely concentrated ring polymers.

MATERIALS AND METHODS

Synthesis of Linear Polymers (lPPA)

Linear poly(phthalaldehyde) was synthesized using anionic polymerization as previously reported.[51] *ortho*-Phthalaldehyde (*o*-PA) monomer was purified using vacuum distillation and subsequently dissolved in anhydrous dichloromethane using a phosphazene base in conjunction with anthracenemethanol. The polymerization was halted upon addition of acetic anhydride, which acts as an end-cap for the polymer ends. The reaction mixture was subsequently precipitated in methanol and dried overnight. Linear PPA polymer was then redissolved in dichloromethane and reprecipitated in methanol, collected, and dried overnight. Polymer samples were stored at −20 °C until further use.

Synthesis of Ring Polymers (cPPA)

Cyclic poly(phthalaldehye) was synthesized as previously reported.[51] *ortho*-Phthalaldehyde monomer was purified via vacuum distillation directly into an air-free reaction vessel, and dissolved in anhydrous dichloromethane. Boron trifluoride diethyerate was added dropwise under mechanical stirring to initiate the polymerization. After 2 h, anhydrous pyridine was added dropwise to quench the reaction. After another 2 h, the reaction products were precipitated in stirred methanol dropwise, collected, and dried overnight. The resultant cPPA ring polymer was dried, redissolved in dichloromethane, and reprecipitated in methanol. Unless otherwise noted, all cPPA samples were stored at −20 °C until further use.

https://doi.org/10.1021/acspolymersau.2c00069
ACS Polym. Au 2023, 3, 307−317

Chemical and Thermal Characterization

^{1}H NMR spectra were obtained with a Varian VXR 500 spectrometer in the School of Chemical Sciences NMR laboratory at the University of Illinois at Urbana−Champaign. Absolute polymer molecular weights were determined via gel permeation chromatography (GPC) (Table 1) with an analytical GPC (Agilent 1200 series) equipped with four Styragel columns (7.8 × 300 mm, HR1, HR3, HR4, and HR5, Waters) coupled to a light scattering module (Wyatt miniDAWN) and a differential refractive index detector (Agilent 1260 Infinity). For absolute molecular weight determination, dn/dc was taken as 0.1515 mL/mg, as previously reported for absolute molecular weight determination from light scattering.[51] We independently confirmed the value of dn/dc using offline refractive index measurements and found agreement within 2%. Thermal gravimetric analysis (TGA) was performed using a TA Instruments Q5000 IR TGA using platinum pans under nitrogen gas flow. Dynamic scans were taken at 10 °C/min scans from 25 to 200 °C. Isothermal experiments were performed at 85 °C.

Sample Preparation for Rheology

Bulk samples of cPPA suitable for rheometry were prepared using a previously reported procedure.[59] Briefly, cPPA and dibutyl phthalate (DBP) are dissolved in HPLC-grade dichloromethane and cast into fluorinated ethylene propylene (FEP)-lined molds, and left to evaporate in an atmosphere partially saturated with dichloromethane vapor overnight. The films were subsequently dried under vacuum for 24 h. Plasticized films were collected and pulverized into thermoforming feedstock powder. The feedstock was then molded into circular discs ≈ 1 mm thick at 85 °C for 10 min using machined aluminum molds of 12.7 mm diameter in an industrial hot-press (Wabash), from which 10 mm discs were subsequently punched out.

Rheometry

Linear viscoelastic (LVE) measurements using shear rheometry on concentrated cPPA samples were performed on an Ares G2 (TA Instruments) with a 10 mm stainless steel parallel plate geometry under nitrogen gas to suppress oxidation of the samples. Despite the use of plasticizer, we recovered the sample after rheometry and found that the mass does not appreciably change (to within <1.8%) after rheological characterization, indicating that evaporation of plasticizer is minimal throughout the test. Strain amplitude sweeps were performed on different samples to ensure access to the linear strain response regime.

Molecular Dynamics Simulations

Polymers are modeled with a semiflexible Kremer-Grest bead−spring model with varying chain length N_b and backbone stiffness k_θ to control the entanglement length.[60,61] All beads have mass m and interact with a purely repulsive Lennard-Jones potential with energy scale ϵ and length-scale σ. Chains are built by connecting beads with finitely extensible nonlinear elastic (FENE) bonds. All simulation quantities are expressed in reduced Lennard-Jones units of length, energy, and time which are σ, ϵ, and $\tau = \sqrt{m\sigma^2/\epsilon}$, respectively. Simulations were run at a constant monomer number density of ρ = 0.85 and a constant temperature $T = \epsilon/k_B$ was maintained by a Langevin thermostat with a thermostat damping time of 100τ. Initial unconcatenated states for concentrated ring melts were generated using the methods of Smrek and co-workers.[41] Unconcatenated ring packings are generated on a lattice and then equilibrated with MD simulations by brute-force for long times. The finitely extensible nonlinear elastic (FENE) bonds of the Kremer-Grest model prevent chains from crossing or forming concatenations during MD simulation.[41] Simulations were run for several billion time steps or until rings diffused by at least three times their size. We carefully monitor equilibration of ring conformations and observe rapid relaxation of their internal distances and gyration tensors on time scales of order the Rouse time for most values of N and k_θ. The exception is the k_θ = 5 system, which develops spontaneous nematic order, and which we exclude from our analyses. In contrast to conformational relaxation, ring COM diffusion was much slower and becomes increasingly suppressed for higher values of N and k_θ. For the highest degrees of polymerization and stiff ring models studied, the final Fickian COM diffusion regime was not achieved, and hence a long-time self-diffusion constant could not be determined. This procedure was possible for all cases except for the longest rings with (N_b = 6400, k_θ = 1.5) and the stiffest rings $k_\theta \geq 4$. Such systems diffuse too slowly to resolve even after several months of continuous simulation on high-performance clusters. Regardless, in all cases, local ring conformations relax much faster than rings diffuse through space, which allows for computation of chain statistics for all systems. Further simulation details are reported in Table S1.

Microscopic Theory

The segmental force level theory for COM diffusion in ring polymer liquids was recently published.[15,38] Additional details relevant to the present application are provided in the Supporting Information (SI).

RESULTS AND DISCUSSION

We began by synthesizing a series of end-capped linear PPA and cyclic poly(phthalaldehyde) cPPA polymer samples (Materials and Methods, Figure 1, Table 1). The largest ring polymers have extremely high molecular weights ($Z = N/N_e$ = 26 and Z = 59) that far exceed prior experiments on stress relaxation in ring polymers based on polystyrene ($Z = N/N_e \lesssim$ 15).[33,34] The glass transition temperature of cPPA ($T_g \approx$ 180 °C) is higher than its degradation temperature $T_d \approx$ 140 °C) (Figures S3−S4),[62] so cPPA samples are plasticized to lower T_g and to enable rheological measurements (Materials and Methods, Figure S5). Moreover, cPPA is thermally stable for hours at temperatures up to 85 °C (Figure S4), which enables linear viscoelastic experiments and time−temperature superposition across a wide temperature range. Films of cPPA were solvent-cast with plasticizer (dibutyl phthalate), and film feedstocks were thermoformed into discs for shear rheometry.[59] During sample processing, any unwanted cleavage of cPPA backbones results in rapid depolymerization to monomer which is monitored by the presence of o-PA monomer in ^{1}H NMR (Figures S6 and S7). To understand the characteristic time scale for cPPA degradation, we performed a series of kinetic degradation experiments by triggering the depolymerization of cPPA using chemical reagents and monitoring depolymerization kinetics via NMR (Figure S8). Our results show that cPPA depolymerization is rapid at ambient temperatures, as indicated by the complete disappearance of the cPPA signal in ^{1}H NMR within 10 s after addition of 10 mM trifluoroacetic acid (Figure S8). Overall, these experiments show that putative cleavage of cPPA backbones is minimal during processing, and any unwanted cleavage of cPPA results in rapid degradation to monomer, thereby avoiding long-lived linear chain contaminants in cPPA samples during rheological characterization.

We next performed linear viscoelastic (LVE) measurements on plasticized cPPA samples containing 58.8 wt % polymer using small amplitude oscillatory shear (SAOS) experiments (Figure S9). Shear rheology was performed across a range of temperatures between 35 and 85 °C, and Williams−Landel−Ferry (WLF) shift factors were determined for the cPPA polymer sample using a reference temperature T_{ref} = 65 °C (Figure S9a). Master curves were then determined for the storage G' and loss moduli G'' (Figure S9b,c). The stress relaxation response $G(t)$ was then determined for plasticized cPPA using Fourier transforms of master curves from linear shear rheology (Figures 2a, S10, SI text). Strikingly, the stress relaxation behavior of the highest MW ring polymer sample (R-1000) exhibits a nearly identical response to the entangled

https://doi.org/10.1021/acspolymersau.2c00069
ACS Polym. Au 2023, 3, 307−317

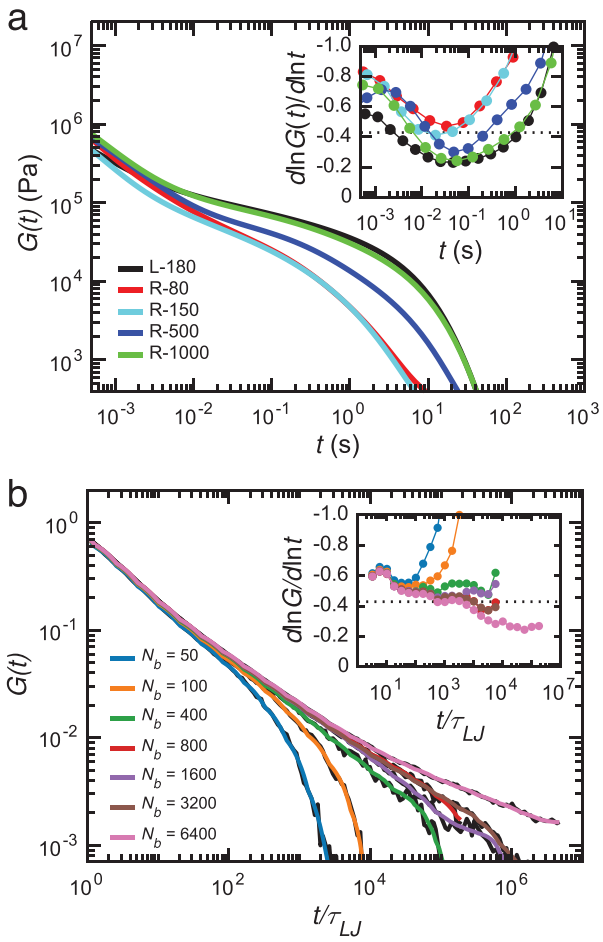

Figure 2. Stress relaxation of linear and ring polymer systems with varying molecular weight. (a) Stress relaxation $G(t)$ master curves from experiments on entangled linear and concentrated cPPA samples as a function of molecular weight (MW). Inset shows derivative slope of $G(t)$ curves, and the dashed line indicates the FLG prediction of $G(t) \propto t^{-3/7}$. Estimates of equivalent $Z = M_w/M_e$ values for the equivalent linear chain for L-180, R-80, R-150, R-500, and R-1000 samples are Z = 10, 4.3, 8.6, 26, and 59, respectively (Table 1 and SI). (b) Stress relaxation $G(t)$ master curves from MD simulations of ring polymer melts with k_θ = 1.5 as a function of N_b. The inset shows slopes of $G(t)$ curves. MD simulation parameters correspond to the canonical Kremer-Grest flexible backbone model with k_θ = 1.5.[16,17] Equivalent N/N_e values for MD simulations with different ring degrees of polymerization N_b and stiffness k_θ = 1.5 are as follows: N_b = 50, 100, 400, 800, 1600, 3200, 6400 corresponds to $Z = N/N_e$ = 1.8, 3.6, 14.3, 28.6, 57.1, 114, 229, respectively, for the equivalent linear chain.

linear polymer of the same chemistry, even though these two polymer samples have different chain topologies and the MW of the linear polymer is 5× smaller than the R-1000 cPPA sample.

Local power-law scaling exponents of the stress relaxation curves (Figure 2a, inset) were determined as $-\,\mathrm{d}\log G(t)/\mathrm{d}\log t$ and unexpectedly show clear deviations from the $G(t) \propto t^{-3/7}$ scaling predicted by the fully diluted FLG model and observed in experiments on LCCC-purified PS ring polymers.[13] At short time scales, the power-law exponent β = 0.5−0.8. At long time scales, the power-law exponent $\beta > 3/7$ for low molecular weight rings but shows a local minimum close to 3/7. However, for high molecular weight rings, the exponent $\beta < 3/7$ over the same range of time scales, and the local minimum is close to $\beta \approx 0.2$, suggesting a slower relaxation process and a possible approach to a dynamical caging state. Prior work on the stress relaxation of relatively low MW LCCC-purified polystyrene rings similarly reported a decreased power-law exponent in the intermediate regime upon intentional addition of linear polymer contaminants in ring polymer melts.[33] However, the self-immolative nature of the cPPA polymer chemistry used in our work precludes the possibility of long-lived linear chain contaminants that would otherwise alter the stress relaxation behavior of pure ring polymer samples.

Molecular dynamics (MD) simulations were used to understand the structure and dynamics of ring polymer melts (Materials and Methods, SI). Coarse-grained MD simulations model polymers as a series of N_b beads connected by finitely extensible nonlinear elastic (FENE) bonds and interacting through a purely repulsive truncated Lennard-Jones potential (Table 2).[16,17] A bending potential $k_\theta(1-\cos(\theta))$ is used to control chain stiffness and the entanglement segment length N_e, where θ is the angle between consecutive bonds. Using this approach, the dynamics of ring polymer melts were simulated at fixed monomer number density ρ = 0.85 for rings of systematically increasing size from $Z \approx 2$, up to extremely high molecular weight (N_b = 6400, corresponding to Z = 230 for the flexible backbone case with k_θ = 1.5), 4× larger than prior MD simulations of ring melts (N_b = 1600, corresponding to Z = 57 with k_θ = 1.5).[16,17] Stress relaxation responses from MD simulations (Figure 2b) show consistent behavior with our experimental results, with the highest MW ring (N_b = 6400) also showing deviation from the power-law stress relaxation decay $t^{-3/7}$ predicted by FLG scaling (Figure 2b), which is consistent with experiments on the high MW ring sample R-1000. Together, experiments and simulations suggest that ring polymers do not obey the constant power-law stress relaxation behavior predicted by prior studies above a critical MW. Moreover, even up to the extremely high degrees of polymerization studied experimentally and with simulation, we find no evidence that the intermediate time dependence of $G(t)$ is approaching a limiting high MW behavior.

A snapshot of flexible ring polymer structure from MD simulation is shown in Figure 3a. Remarkably, results from MD simulations show that high MW ring polymers are highly porous and strongly interpenetrate with neighboring rings in concentrated systems. Average intramolecular monomer

Table 2. Parameters for MD Simulations of Ring Polymers Used in This Work[a]

N_b	k_θ	N_e	Z
800	1.5	28	29
1600	1.5	28	57
3200	1.5	28	114
6400	1.5	28	229
1600	0	84	19
1600	2.0	20.5	78
1600	2.25	18	90
1600	3.0	13	121
1600	4.0	11	145

[a] N_b is the number of beads per chain, k_θ is the bending potential of the chain, N_e is the entanglement segment length, and $Z = N/N_e$ is the number of entanglements per equivalent linear chain.[63]

https://doi.org/10.1021/acspolymersau.2c00069
ACS Polym. Au 2023, 3, 307−317

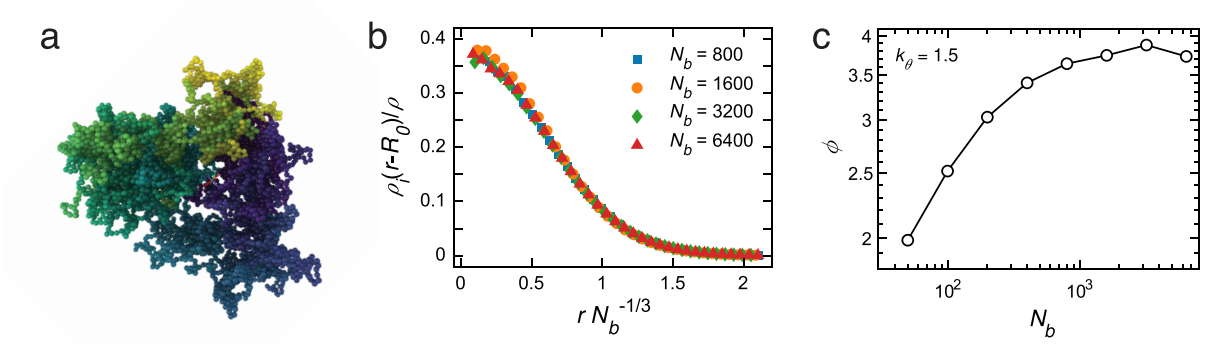

Figure 3. Ring polymers are highly porous structures in concentrated ring systems. (a) Snapshot of ring polymer conformation showing a single ring in a dense melt from equilibrated MD simulations for N_b = 6400 and k_θ = 1.5. Coarse-grained atoms are colored sequentially along the ring backbone from purple to green to yellow. (b) Intramolecular monomer density as a function of distance from the center-of-mass of a ring scaled by its radius-of-gyration R_g for different ring molecular weights N_b with k_θ = 1.5. (c) Macromolecular volume fraction $\phi = 4\pi\rho R_g^3/3N_b$ for a flexible ring polymer with k_θ = 1.5, where ρ is the total monomer or bead number density. Equivalent $Z = N/N_e$ values for MD simulations with different chain sizes N_b and k_θ = 1.5 are as follows: N_b = 800, 1600, 3200, 6400 corresponds to $Z = N/N_e$ = 28.6, 57.1, 114, 229, respectively, for the equivalent linear chain.

density for rings relative to their center-of-mass is plotted in Figure 3b for different ring molecular weights with fixed stiffness (k_θ = 1.5, corresponding to a typical flexible polymer backbone[16]). Notably, the average conformations of concentrated rings are quite spherical and densest at their center-of-mass. Rings of different lengths show similar intramolecular density profiles when r is scaled by $N^{-1/3}$. The scaled data in Figure 3b also show that high MW rings maintain a similar shape with global fractal dimension 3 as molecular weight increases. Intramolecular monomer density shows that only ≈40% of monomers belonging to the same ring polymer are located near the ring center-of-mass, indicating that on average, the core of each ring polymer is comprised of ≈60% monomers belonging to other nearby ring polymers in the melt. Figure 3c shows the macromolecular volume fraction $\phi = 4\pi\rho R_g^3/3N_b$ as a function of molecular weight for equilibrated MD ring polymers at a fixed backbone stiffness (bending parameter k_θ = 1.5), where ρ is monomer number density. We note that the macromolecular volume fraction ϕ is analogous to the scaled polymer concentration c/c^* in linear chain polymer liquids, where c^* is the polymer overlap concentration, a standard parameter used to quantify degree of interpenetration in polymeric liquids. At the highest molecular weights (N_b > 1600), $\phi \approx 3.7$ and increases from $2.0 \lesssim \phi \lesssim 4.0$ from the lowest molecular weights (N_b < 800). Overall, these results suggest that ring polymers are globally compact yet highly porous structures and strongly interpenetrate in concentrated systems. Therefore, ring−ring interactions cannot be neglected when considering the dynamics of individual ring polymers.

To capture the effects of strong intermolecular interactions, a segmental scale force level theory was recently developed for some aspects of ring dynamics by combining concepts from polymer, liquid state, and glass physics.[15,38] The theory enables predictions of the COM diffusion constant D, the longest conformational relaxation time, and the intermediate-time non-Fickian transport of dense ring polymer solutions and melts.[15,38] The essential idea is that high MW rings behave like fluctuating soft particles that strongly interpenetrate. The interpenetration of neighboring rings imposes dynamic constraints on their motion due to long-lived correlations in intermolecular excluded volume forces,[15,38] which could be supported by recent observations of intermediate-time anomalous diffusion dynamics in ring polymers studied by neutron spin echo and pulsed-field NMR experiments.[45] The key variable is N/N_D, where N is the segmental degree of polymerization of the adopted coarse-grained ring model and N_D quantifies a dynamic crossover beyond which intermolecular effects are nonperturbative and control slow ring dynamics. Based on a 2-fractal scaling model of ring intramolecular structure that encodes topological compaction effects associated with the linear chain equivalent entanglement length scale and N_e, the combined structural and dynamical theories predict that the crucial quantity is $N_D \approx 9\pi S_0\phi/1.17 \propto \phi^{-3/2}$. Here, ϕ quantifies the degree of inter-ring interpenetration and S_0 is the dimensionless compressibility (i.e., the inverse of which is a measure of inter-ring excluded volume induced dynamical constraints). The quantities ϕ and S_0 depend on polymer chemistry and backbone stiffness or Kuhn length. For the COM diffusion constant D, unentangled Rouse ($D \sim N^{-1}$ for $N < N_D$), weakly caged ($D \sim N_D/N^2$ for $N_D < N < N_{on}$), and strongly caged activated hopping ($D \sim (N_D/N^2)\exp(-\alpha[N/N_{on} - b])$ for $N > N_{on} > N_D$, where b is a parameter slightly larger than unity) regimes are predicted with increasing N, where α is a $O(1)$ constant. Quantitative comparisons with simulation data of D for flexible and semiflexible ring melt and dense solution models, and also for the intermediate time COM mean-squared displacement of flexible ring melts, are in good agreement with the theory in the weak caging regime based on the identification $N = N_b$.[15,38] Importantly, the intermediate non-Fickian time-dependence is predicted to change at a length scale on the order of the linear chain entanglement length because it is at this scale that the single ring conformations (and inter-ring packing correlations) cross over from ideal coils to compact globules due to static topological effects. For degrees of polymerization N larger than a critical onset degree of polymerization (estimated as $N_{on} \approx 4.35N_D$ for a specific simulation model), an even slower dynamical regime emerges where COM motion becomes transiently localized and there is a smooth crossover to activated dynamics.[38] Quantitative analysis of simulations of the COM diffusion constant of dense solutions of semiflexible rings provide support for the idea of a second crossover to an activated transport regime.[38] Moreover, we emphasize that our

https://doi.org/10.1021/acspolymersau.2c00069
ACS Polym. Au 2023, 3, 307−317

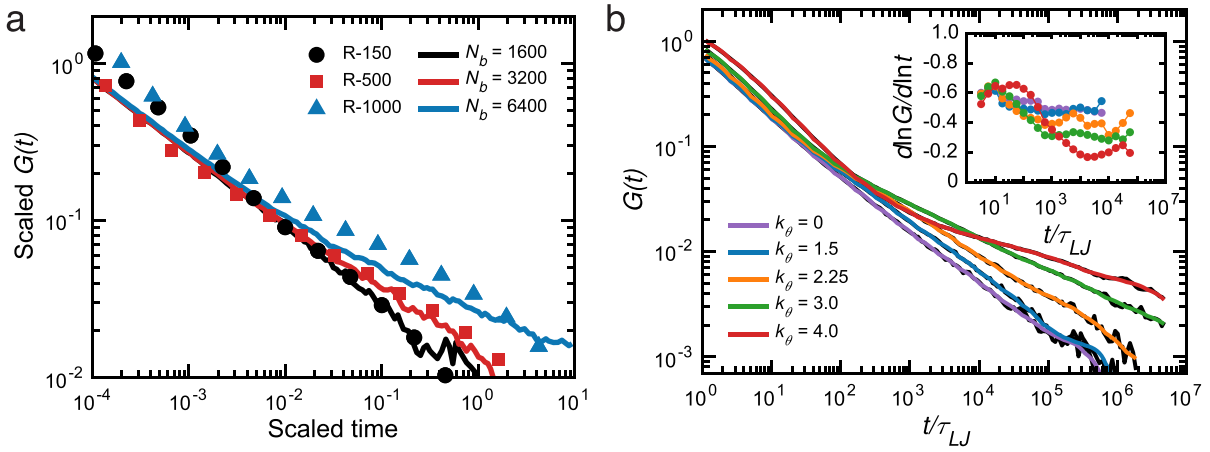

Figure 4. Comparison of ring polymer stress relaxation from experiments and MD simulations. (a) Scaled $G(t)$ stress relaxation curves from experiments (symbols) and MD simulations (lines) as a function of N_b with $k_\theta = 1.5$. Estimates of equivalent Z values for the equivalent linear chain for R-150, R-500, and R-1000 samples are $Z = 8.6$, 26, and 59, respectively (Table 1 and SI). Equivalent Z values for MD simulations with different chain sizes N_b and $k_\theta = 1.5$ are as follows: $N_b = 1600$, 3200, 6400 corresponds to $Z = N/N_e = 57.1$, 114, 229, respectively, for the equivalent linear chain. (b) Stress relaxation curves $G(t)$ from MD simulations at a fixed molecular weight $N_b = 1600$ for polymers with varying bending stiffness k_θ. Curves in black denote raw data and colored lines indicate Savitzky-Golay filtered data. Inset shows derivative slope of $G(t)$ curves as a function of dimensionless time. Equivalent Z values for MD simulations with $N_b = 1600$ and $k_\theta = 0$, 1.5, 2.25, 3.0, 4.0 are as follows: $Z = 19$, 57, 90, 121, 145, respectively, for the equivalent linear chain (Table 2).

simulation results suggest that (in qualitative contrast to entangled linear chains) ring COM diffusion is much slower than conformational relaxation, and increasingly so as ring molecular weight and stiffness increase. Taken together, these results imply a strong decoupling of internal relaxation and mass transport. This physical behavior is at the core of the self-consistent (beyond weak caging) theory[38] that predicts a crossover to glassy-like activated dynamics.

Extension of this theoretical approach to quantitatively predict how intermolecular correlated forces modify ring internal dynamic modes and stress relaxation has not yet been achieved. Hence, the existing theory cannot make direct predictions for $G(t)$ that is the focus of our present work. However, as a working hypothesis we conjecture that the slowing down of COM motion and the longest conformational relaxation time due to many ring dynamical caging effects will disrupt the self-similar relaxation of rings and modify their stress relaxation $G(t)$, thereby giving rise to non-power-law stress relaxation behavior. It is important to note that the caging physics included in the microscopic model is predicted to suppress ring polymer COM motion on length and time scales smaller than the ring polymer size R_g. In other words, the theory for COM motion accounts for new physics at time scales and length scales starting far inside the macromolecular length scale R_g. This approach considers forces at *microscopic* length and time scales and resolves their influence on dynamics at larger length scales. The longest FLG relaxation time scale can only be related to dynamics at smaller length and time scales through self-similar scaling arguments, which rely upon the assumption that the only relevant scales are the fundamental loop size and the chain size. On the other hand, a general feature of dynamic caging is that it constrains motions at length scales far smaller than the polymer size R_g. This produces a new scale of dynamic confinement that is expected—quite generally—to disrupt the power-law self-similar relaxation spectrum predicted by dynamic scaling models such as FLG.[38] Broadly, these ideas seem to be qualitatively consistent with the observed slow-down in the stress relaxation behavior in our experiments and simulations.

To tentatively explore the above hypothesis in the present context in a semiquantitative manner, we consider as a crude criterion for the breakdown of the FLG model for $G(t)$ as when the predicted ring COM hopping time τ_{hop} exceeds the characteristic longest conformational or stress relaxation time of the FLG model:

$$\tau_{hop} > \gamma\tau_{FLG}$$

where γ is a $O(1)$ constant. Of course, this criterion is not rigorous, but rather reflects the qualitative idea that if the longest relaxation time from the FLG model τ_{FLG} is smaller than the time scale for hopping τ_{hop}, it would seem inevitable that the new inter-ring caging physics is relevant in the intermediate time scale regime where our experiments and simulations find strong deviations of $G(t)$ from the FLG model predicted form. Conveniently, both the FLG model[13] and the microscopic theory[38] have been previously parametrized to predict relaxation times for analogous bead−spring models, such as the flexible ring melt studied in this work. Using the microscopic theory previously parametrized for our ring simulations to compute the hopping time τ_{hop}, identifying $N = N_b$ for the fully flexible bead−spring model, and using the known expression for the FLG longest relaxation time τ_{FLG},[13] we can determine an onset degree of polymerization N^* such that $\tau_{hop} > \gamma\tau_{FLG}$ (SI). Numerical solution for the simulated flexible ring polymer model ($k_\theta = 1.5$, Figure 2b) yields $N^* = 930$, 1100, 1190 for $\gamma = 1$, 2, 3. Although we do not wish to overemphasize the quantitative values, the consistency to within a factor of 3 of these predicted values of N_b^* with the onset of deviations of the form of $G(t)$ from the FLG model and the emergence of slow relaxation behavior observed in our experiments and simulations (beginning at $N_b \approx 3200$ in the simulations) seems consistent with our theory-based hypothesis. The theory predicts that because increasing ring polymer molecular weight or backbone stiffness (which correlates with

https://doi.org/10.1021/acspolymersau.2c00069
ACS Polym. Au 2023, 3, 307−317

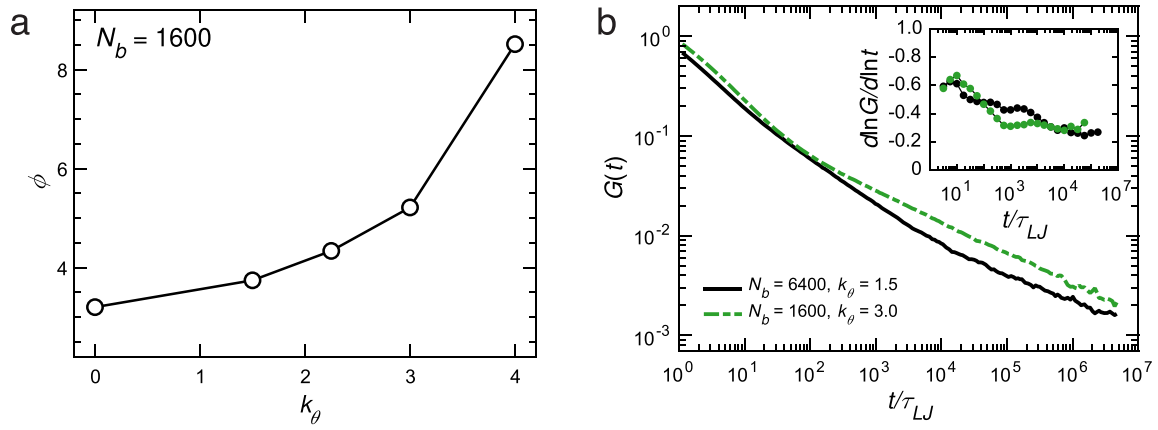

Figure 5. Macromolecular volume fraction and stress relaxation dynamics for ring polymers with different backbone stiffnesses and molecular weights. (a) Macromolecular volume fraction ϕ dependence on bending stiffness k_θ at a fixed N_b = 1600. (b) Comparison of stress relaxation $G(t)$ from MD simulations with N_b = 1600, k_θ = 3.0 and N_b = 6400, k_θ = 1.5 stress relaxation curves showing similar behavior and deviations away from FLG scaling predictions for intermediate time stress relaxation.

a decrease of N_e) enhances ring polymer-ring interpenetration, the ring polymer COM diffusion slows down.

To test these ideas, we first examined the effect of ring polymer molecular weight on stress relaxation for polymers with fixed backbone stiffness. Figure 4a shows a comparison between stress relaxation from cPPA experiments and MD simulations for rings with N_b = 1600, 3200, 6400 with fixed backbone stiffness k_θ = 1.5. When the stress relaxation curves and time scales are appropriately scaled, reasonable agreement is achieved between the highest cPPA molecular weights in experiments (R-500 and R-1000) and the largest MW rings in MD simulations N_b = 3200 and 6400. As discussed in the SI (section 1.5), there is good accord between the experimental and simulation degrees of polymerization in this comparison.

We next examined the effects of increasing backbone stiffness on ring polymer dynamics. Changes in polymer backbone stiffness lead to changes in the macromolecular volume fraction ϕ, which in turn give rise to changes in the key variable N/N_D. Specifically, at fixed density, N_D is predicted to decrease with increasing ring stiffness due to increasing macromolecular volume fraction ϕ. MD simulations provide a facile method to vary polymer backbone stiffness, which is challenging to do in experiments without changing polymer chemistry. Figure 4b shows the effects of changing backbone stiffness on the dynamics of ring polymers at a fixed molecular weight N_b = 1600 from MD simulations. As polymer backbone stiffness increases, and hence N/N_D increases at fixed ring molecular weight, the stress relaxation behavior significantly slows down. Nonuniversal stress relaxation dynamics are clearly observed in the stress relaxation curves, such that the local power-law slopes tend toward smaller magnitudes with increasing stiffness with no evidence of approaching a limiting small value (Figure 4b, inset).

The MD results for varying MW and stiffness are qualitatively consistent with the ideas employed in the microscopic theory.[15,38] Figure 5a shows the macromolecular volume fraction ϕ as a function of backbone stiffness at fixed N_b = 1600. In contrast to the ϕ dependence on N_b shown in Figure 3c, ϕ sharply increases for $k_\theta > 1.5$. At k_θ = 3.0, $\phi \approx 5.2$, which is well above the maximum ϕ observed for increasing N_b ($\phi \approx 3.8$, Figure 3c). Simply doubling the polymer backbone stiffness increases the amount of interpenetration in the N_b = 1600 ring polymer case by ≈40%, whereas quadrupling the molecular weight essentially maintains the same number of molecules per volume (Figure 3c). One thus expects that increasing N and increasing stiffness will both lead to larger values of N/N_D. Hence, the ideas from theory suggest it should be possible to find a pair of values of stiffness k_θ and N (or N_b) that have similar values of N/N_D (or N_b/N_D). Then the question is whether this condition correlates with observing similar ring dynamics, including $G(t)$.

To explore the above scenario, we used MD simulations to determine whether stress relaxation dynamics for polymers with different backbone stiffnesses and molecular weights can be similar. Figure 5b shows a direct comparison of the stress relaxation behavior for a semiflexible ring (N_b = 1600, k_θ = 3.0) and a flexible ring polymer with higher MW (N_b = 6400, k_θ = 1.5). Reasonable agreement is achieved for the intermediate stress relaxation behavior for the two different systems, including nearly identical values of the minimum power law exponent exhibited by $G(t)$ (Figure 5b, inset).This result also suggests that comparisons between a different polymer chemistry to a more well-studied system (e.g., polystyrene, with simulation parameters k_θ = 1.5) are reasonable. Overall, these results suggest that the microscopic theory provides qualitative support for the intriguing simulation results in Figure 5b and the proposition that N/N_D is an important physical metric (perhaps not the only one) quantifying the influence of inter-ring interactions on slow dynamics. In other words, describing the stress relaxation dynamics using the number of entanglements per equivalent linear chain $Z = N/N_e$ (or $Z = N_b/N_e$) does not lead to universal behavior, as the observed relaxation scalings vary for different backbone stiffnesses even at similar Z ($N_e \approx 28$ and ≈17 for k_θ = 1.5 and 3.0, respectively). Quantitative theoretical analysis requires going beyond the prior work of refs15 and 38, to include in a general manner the effect of backbone stiffness and N_e on the intraring structure factor, which is the key input to the theory of packing structure and dynamics, and thus the ability to quantitatively predict the dynamic crossover N_D. Work in this direction is currently in progress.

CONCLUSION

In this work, we report the unexpected nonuniversal stress relaxation dynamics of high MW ring polymers. Although prior

https://doi.org/10.1021/acspolymersau.2c00069
ACS Polym. Au 2023, 3, 307−317

experiments and simulations appear to show good agreement with a self-similar power-law relaxation until terminal relaxation, our work reports fundamentally new physics for extremely high MW rings, together with unprecedented levels of ring polymer purity. We observe a slowdown in stress relaxation dynamics for pure ring polymer systems using a self-immolative polymer chemistry, and experimental results are complemented by MD simulations of ring polymers. In addition, a recently developed force level theory for the COM dynamics and terminal relaxation time of ring polymer liquids is used to estimate the onset of nonuniversal and non-power-law stress relaxation dynamics, and the results are qualitatively consistent with results from MD simulations of extremely high MW ring polymers. Broadly, our results show that the new physics uncovered in this work cannot be solely explained by the number of entanglements of the equivalent linear chain $Z = N/N_e$. Rather, we believe that explicit intermolecular dynamical effects associated with N and stiffness dependent ring−ring interpenetration are crucial.

Overall, the combination of new experiments, simulations, and theory in this work sheds new light on the nontrivial physics in densely packed ring liquids and suggests the importance of intermolecular interactions and space-time force correlations in ring polymer liquids. Moving forward, our work holds clear implications for the future development of molecular theories of ring polymer dynamics. In particular, there is a need for theoretical frameworks that can be generalized to treat ring polymer internal modes which will allow explicit prediction of the segmental mean-squared displacement and $G(t)$, allowing for detailed comparison to simulations and experiments. Future experiments can be designed to systematically understand the role of backbone stiffness using different chemistries, in addition to understanding the role of ring-linear blends on dynamics.

■ ASSOCIATED CONTENT

Supporting Information

The Supporting Information is available free of charge at https://pubs.acs.org/doi/10.1021/acspolymersau.2c00069.

Additional experimental procedures, supplemental text, DMA, GPC and size exclusion chromatography, TGA, NMR data, linear rheology, MD simulation parameters and some details of the theoretical analysis (PDF)

■ AUTHOR INFORMATION

Corresponding Authors

Thomas C. O'Connor − *Department of Materials Science and Engineering, Carnegie Mellon University, Pittsburgh, Pennsylvania 15213, United States;* orcid.org/0000-0002-9393-0295; Email: thomaso@andrew.cmu.edu

Charles M. Schroeder − *Department of Materials Science and Engineering, Department of Chemical and Biomolecular Engineering, Beckman Institute for Advanced Science and Technology, Department of Chemistry, and Materials Research Laboratory, University of Illinois at Urbana−Champaign, Urbana, Illinois 61801, United States;* orcid.org/0000-0001-6023-2274; Email: cms@illinois.edu

Authors

Michael Q. Tu − *Department of Chemical and Biomolecular Engineering and Beckman Institute for Advanced Science and Technology, University of Illinois at Urbana−Champaign, Urbana, Illinois 61801, United States*

Oleg Davydovich − *Department of Chemistry and Beckman Institute for Advanced Science and Technology, University of Illinois at Urbana−Champaign, Urbana, Illinois 61801, United States;* orcid.org/0000-0002-1096-7034

Baicheng Mei − *Department of Materials Science and Engineering and Materials Research Laboratory, University of Illinois at Urbana−Champaign, Urbana, Illinois 61801, United States;* orcid.org/0000-0003-0289-248X

Piyush K. Singh − *Department of Chemical and Biomolecular Engineering and Beckman Institute for Advanced Science and Technology, University of Illinois at Urbana−Champaign, Urbana, Illinois 61801, United States*

Gary S. Grest − *Sandia National Laboratories, Albuquerque, New Mexico 87185, United States;* orcid.org/0000-0002-5260-9788

Kenneth S. Schweizer − *Department of Materials Science and Engineering, Department of Chemical and Biomolecular Engineering, Beckman Institute for Advanced Science and Technology, Department of Chemistry, and Materials Research Laboratory, University of Illinois at Urbana−Champaign, Urbana, Illinois 61801, United States*

Complete contact information is available at: https://pubs.acs.org/10.1021/acspolymersau.2c00069

Author Contributions

CRediT: **Michael Q. Tu** conceptualization (equal), data curation (equal), formal analysis (equal), investigation (equal), writing-original draft (equal), writing-review & editing (equal); **Oleg Davydovich** data curation (equal), formal analysis (equal), investigation (equal), writing-original draft (equal); **Baicheng Mei** formal analysis (equal), investigation (equal), writing-original draft (equal); **Piyush K. Singh** data curation (equal), investigation (equal), writing-original draft (equal); **Gary S. Grest** conceptualization (equal), data curation (equal), software (equal), writing-original draft (equal); **Kenneth S. Schweizer** conceptualization (equal), formal analysis (equal), funding acquisition (equal), investigation (equal), supervision (equal), writing-original draft (equal), writing-review & editing (equal); **Thomas C. O'Connor** conceptualization (equal), formal analysis (equal), investigation (equal), software (equal), writing-original draft (equal), writing-review & editing (equal); **Charles M. Schroeder** conceptualization (equal), funding acquisition (equal), investigation (equal), project administration (equal), supervision (equal), writing-original draft (equal), writing-review & editing (equal).

Notes

The authors declare no competing financial interest.

■ ACKNOWLEDGMENTS

This work was funded by the National Science Foundation (NSF) Awards CBET-1604038 (M.Q.T. and C.M.S.), the Joint Center for Energy Storage Research (JCESR), an Energy Innovation Hub funded by the U.S. Department of Energy, Office of Sciences (M.Q.T. and C.M.S.), and a Sandia Academic Alliance Fellowship (M.Q.T. and C.M.S.). T.C.O. acknowledges startup funding from Carnegie Mellon University. This work was performed, in part, at the Center for Integrated Nanotechnologies, an Office of Science User Facility operated for the U.S. Department of Energy (DOE)

Office of Science. Sandia National Laboratories is a multimission laboratory managed and operated by National Technology & Engineering Solutions of Sandia, LLC, a wholly owned subsidiary of Honeywell International, Inc., for the U.S. DOE's National Nuclear Security Administration under Contract No. DE-NA0003525. The views expressed in the article do not necessarily represent the views of the U.S. DOE or the U.S. Government. We thank Simon Rogers, Johnny Ching-Wei Lee, Jeffrey Moore, and Christopher Rudolphi for useful discussions and assistance with experiments and Jan Smrek with assistance with simulations.

REFERENCES

(1) Doi, M.; Edwards, S. F. *The Theory of Polymer Dynamics*; Oxford University Press, 1988; Vol. 73.
(2) McLeish, T.; Larson, R. Molecular Constitutive Equations for A Class of Branched Polymers: the Pom-Pom Polymer. *J. Rheol.* **1998**, *42*, 81−110.
(3) McLeish, T.; et al. Dynamics of Entangled H-Polymers: Theory, Rheology, and Neutron-Scattering. *Macromolecules* **1999**, *32*, 6734−6758.
(4) Milner, S. T.; McLeish, T. Parameter-Free Theory for Stress Relaxation in Star Polymer Melts. *Macromolecules* **1997**, *30*, 2159−2166.
(5) De Gennes, P. Reptation of Stars. *J. Phys. (Paris)* **1975**, *36*, 1199−1203.
(6) McLeish, T. Floored by the Rings. *Nat. Mater.* **2008**, *7*, 933−935.
(7) Rao, S. S.; Huntley, M. H.; Durand, N. C.; Stamenova, E. K.; Bochkov, I. D.; Robinson, J. T.; Sanborn, A. L.; Machol, I.; Omer, A. D.; Lander, E. S.; Aiden, E. L. A 3D Map of the Human Genome at Kilobase Resolution Reveals Principles of Chromatin Looping. *Cell* **2014**, *159*, 1665−1680.
(8) Cairns, J. The Bacterial Chromosome and Its Manner of Replication As Seen by Autoradiography. *J. Mol. Biol.* **1963**, *6*, 208−IN5.
(9) Ferraro, B.; Morrow, M. P.; Hutnick, N. A.; Shin, T. H.; Lucke, C. E.; Weiner, D. B. Clinical Applications of DNA Vaccines: Current Progress. *Clinical Infectious Diseases* **2011**, *53*, 296−302.
(10) Wu, Q.; Rauscher, P. M.; Lang, X.; Wojtecki, R. J.; de Pablo, J. J.; Hore, M. J. A.; Rowan, S. J. Poly[n]catenanes: Synthesis of molecular interlocked chains. *Science* **2017**, *358*, 1434−1439.
(11) Rauscher, P. M.; Schweizer, K. S.; Rowan, S. J.; de Pablo, J. J. Dynamics of poly[n]catenane melts. *J. Chem. Phys.* **2020**, *152*, 214901.
(12) Rubinstein, M. Dynamics of Ring Polymers in the Presence of Fixed Obstacles. *Phys. Rev. Lett.* **1986**, *57*, 3023.
(13) Ge, T.; Panyukov, S.; Rubinstein, M. Self-Similar Conformations and Dynamics in Entangled Melts and Solutions of Nonconcatenated Ring Polymers. *Macromolecules* **2016**, *49*, 708−722.
(14) Dell, Z. E.; Schweizer, K. S. Intermolecular Structural Correlations in Model Globular and Unconcatenated Ring Polymer Liquids. *Soft Matter* **2018**, *14*, 9132−9142.
(15) Mei, B.; Dell, Z. E.; Schweizer, K. S. Microscopic Theory of Long-Time Center-of-Mass Self-Diffusion and Anomalous Transport in Ring Polymer Liquids. *Macromolecules* **2020**, *53*, 10431−10445.
(16) Halverson, J. D.; Lee, W. B.; Grest, G. S.; Grosberg, A. Y.; Kremer, K. Molecular Dynamics Simulation Study of Nonconcatenated Ring Polymers in A Melt. I. Statics. *J. Chem. Phys.* **2011**, *134*, 204904.
(17) Halverson, J. D.; Lee, W. B.; Grest, G. S.; Grosberg, A. Y.; Kremer, K. Molecular Dynamics Simulation Study of Nonconcatenated Ring Polymers in A Melt. II. Dynamics. *J. Chem. Phys.* **2011**, *134*, 204905.
(18) Tsalikis, D. G.; Mavrantzas, V. G.; Vlassopoulos, D. Analysis of Slow Modes in Ring Polymers: Threading of Rings Controls Long-Time Relaxation. *ACS Macro Lett.* **2016**, *5*, 755−760.
(19) Schroeder, C. M. Single Polymer Dynamics for Molecular Rheology. *J. Rheol.* **2018**, *62*, 371−403.
(20) Li, Y.; Hsiao, K.-W.; Brockman, C. A.; Yates, D. Y.; Robertson-Anderson, R. M.; Kornfield, J. A.; San Francisco, M. J.; Schroeder, C. M.; McKenna, G. B. When Ends Meet: Circular DNA Stretches Differently in Elongational Flows. *Macromolecules* **2015**, *48*, 5997−6001.
(21) Hsiao, K.-W.; Schroeder, C. M.; Sing, C. E. Ring Polymer Dynamics Are Governed by a Coupling between Architecture and Hydrodynamic Interactions. *Macromolecules* **2016**, *49*, 1961−1971.
(22) Tu, M. Q.; Lee, M.; Robertson-Anderson, R. M.; Schroeder, C. M. Direct Observation of Ring Polymer Dynamics in the Flow-Gradient Plane of Shear Flow. *Macromelecules* **2020**, *53*, 9406−9419.
(23) Zhou, Y.; Hsiao, K.-W.; Regan, K. E.; Kong, D.; McKenna, G. B.; Robertson-Anderson, R. M.; Schroeder, C. M. Effect of molecular architecture on ring polymer dynamics in semidilute linear polymer solutions. *Nat. Commun.* **2019**, *10*, 1753.
(24) Zhou, Y.; Young, C. D.; Lee, M.; Banik, S.; Kong, D.; McKenna, G. B.; Robertson-Anderson, R. M.; Sing, C. E.; Schroeder, C. M. Dynamics and Rheology of Ring-Linear Blend Semidilute Solutions in Extensional Flow: Single Molecule Experiments. *J. Rheol.* **2021**, *65*, 729−744.
(25) Young, C. D.; Zhou, Y.; Schroeder, C. M.; Sing, C. E. Dynamics and Rheology of Ring-Linear Blend Semidilute Solutions in Extensional Flow: Modeling and Molecular Simulations. *J. Rheol.* **2021**, *65*, 757−777.
(26) Doi, Y.; Matsumoto, A.; Inoue, T.; Iwamoto, T.; Takano, A.; Matsushita, Y.; Takahashi, Y.; Watanabe, H. Re-Examination of Terminal Relaxation Behavior of High-Molecular-Weight Ring Polystyrene Melts. *Rheol. Acta* **2017**, *56*, 567−581.
(27) McKenna, G.; Hadziioannou, G.; Lutz, P.; Hild, G.; Strazielle, C.; Straupe, C.; Rempp, P.; Kovacs, A. Dilute Solution Characterization of Cyclic Polystyrene Molecules and Their Zero-Shear Viscosity in the Melt. *Macromolecules* **1987**, *20*, 498−512.
(28) Lee, H. C.; Lee, H.; Lee, W.; Chang, T.; Roovers, J. Fractionation of Cyclic Polystyrene From Linear Precursor by HPLC at the Chromatographic Critical Condition. *Macromolecules* **2000**, *33*, 8119−8121.
(29) Molnar, K.; Helfer, C. A.; Kaszas, G.; Krisch, E.; Chen, D.; McKenna, G. B.; Kornfield, J. A.; Puskas, J. E. Liquid Chromatography at Critical Conditions (LCCC): Capabilities and Limitations for Polymer Analysis. *J. Mol. Liq.* **2021**, *322*, 114956.
(30) Yan, Z.-C.; Costanzo, S.; Jeong, Y.; Chang, T.; Vlassopoulos, D. Linear and Nonlinear Shear Rheology of A Marginally Entangled Ring Polymer. *Macromolecules* **2016**, *49*, 1444−1453.
(31) Parisi, D.; Costanzo, S.; Jeong, Y.; Ahn, J.; Chang, T.; Vlassopoulos, D.; Halverson, J. D.; Kremer, K.; Ge, T.; Rubinstein, M.; et al. Nonlinear Shear Rheology of Entangled Polymer Rings. *Macromolecules* **2021**, *54*, 2811−2827.
(32) Huang, Q.; Ahn, J.; Parisi, D.; Chang, T.; Hassager, O.; Panyukov, S.; Rubinstein, M.; Vlassopoulos, D. Unexpected Stretching of Entangled Ring Macromolecules. *Phys. Rev. Lett.* **2019**, *122*, 208001.
(33) Kapnistos, M.; Lang, M.; Vlassopoulos, D.; Pyckhout-Hintzen, W.; Richter, D.; Cho, D.; Chang, T.; Rubinstein, M. Unexpected Power-Law Stress Relaxation of Entangled Ring Polymers. *Nat. Mater.* **2008**, *7*, 997−1002.
(34) Doi, Y.; Matsubara, K.; Ohta, Y.; Nakano, T.; Kawaguchi, D.; Takahashi, Y.; Takano, A.; Matsushita, Y. Melt Rheology of Ring Polystyrenes with Ultrahigh Purity. *Macromolecules* **2015**, *48*, 3140−3147.
(35) Pasquino, R.; et al. Viscosity of Ring Polymer Melts. *ACS Macro Lett.* **2013**, *2*, 874−878.
(36) Smrek, J.; Grosberg, A. Y. Understanding the Dynamics of Rings in the Melt in Terms of the Annealed Tree Model. *J. Phys.: Condens. Matter* **2015**, *27*, 064117.
(37) Sakaue, T. Topological free volume and quasi-glassy dynamics in the melt of ring polymers. *Soft Matter* **2018**, *14*, 7507−7515.

https://doi.org/10.1021/acspolymersau.2c00069
ACS Polym. Au 2023, 3, 307−317

(38) Mei, B.; Dell, Z. E.; Schweizer, K. S. Theory of Transient Localization, Activated Dynamics, and a Macromolecular Glass Transition in Ring Polymer Liquids. *ACS Macro Lett.* **2021**, *10*, 1229−1235.
(39) Michieletto, D.; Turner, M. S. A Topologically Driven Glass in Ring Polymers. *Proc. Natl. Acad. Sci. U. S. A.* **2016**, *113*, 5195−5200.
(40) Michieletto, D.; Nahali, N.; Rosa, A. Glassiness and Heterogeneous Dynamics in Dense Solutions of Ring Polymers. *Phys. Rev. Lett.* **2017**, *119*, 197801.
(41) Smrek, J.; Kremer, K.; Rosa, A. Threading of Unconcatenated Ring Polymers at High Concentrations: Double-Folded vs Time-Equilibrated Structures. *ACS Macro Lett.* **2019**, *8*, 155−160.
(42) Ubertini, M. A.; Smrek, J.; Rosa, A. Entanglement Length Scale Separates Threading from Branching of Unknotted and Non-concatenated Ring Polymers in Melts. *Macromolecules* **2022**, *55*, 10723−10736.
(43) Götze, W. *Complex dynamics of glass-forming liquids: A mode-coupling theory*; Oxford University Press, 2009; Vol. *143*.
(44) Schweizer, K. S.; Curro, J. G. Integral equation theories of the structure, thermodynamics, and phase transitions of polymer fluids. In *Advances in Chemical Physics*; Prigogine, I., Rice, S. A., Eds.; Wiley, 1997; Vol. *98*, p 1.
(45) Kruteva, M.; Monkenbusch, M.; Allgaier, J.; Holderer, O.; Pasini, S.; Hoffmann, I.; Richter, D. Self-Similar Dynamics of Large Polymer Rings: A Neutron Spin Echo Study. *Phys. Rev. Lett.* **2020**, *125*, 238004.
(46) Lutz, J. P.; Davydovich, O.; Hannigan, M. D.; Moore, J. S.; Zimmerman, P. M.; McNeil, A. J. Functionalized and Degradable Polyphthalaldehyde Derivatives. *J. Am. Chem. Soc.* **2019**, *141*, 14544−14548.
(47) Aso, C.; Tagami, S.; Kunitake, T. Polymerization of Aromatic Aldehydes. II. Cationic Cyclopolymerization of Phthalaldehyde. *Journal of Polymer Science Part A-1: Polymer Chemistry* **1969**, *7*, 497−511.
(48) Aso, C.; Tagami, S. Polymerization of Aromatic Aldehydes. III. The Cyclopolymerization of Phthaldehyde and the Structure of the Polymer. *Macromolecules* **1969**, *2*, 414−419.
(49) Seo, W.; Phillips, S. T. Patterned Plastics That Change Physical Structure in Response To Applied Chemical Signals. *J. Am. Chem. Soc.* **2010**, *132*, 9234−9235.
(50) Willson, C. G.; Ito, H.; Frechet, J. M. J.; Tessier, T. G.; Houlihan, F. M. Approaches to the Design of Radiation-Sensitive Polymeric Imaging Systems with Improved Sensitivity and Resolution. *J. Electrochem. Soc.* **1986**, *133*, 181.
(51) Kaitz, J. A.; Diesendruck, C. E.; Moore, J. S. End Group Characterization of Poly (Phthalaldehyde): Surprising Discovery of A Reversible, Cationic Macrocyclization Mechanism. *J. Am. Chem. Soc.* **2013**, *135*, 12755−12761.
(52) Roovers, J.; Toporowski, P. Synthesis of High Molecular Weight Ring Polystyrenes. *Macromolecules* **1983**, *16*, 843−849.
(53) Roovers, J.; Toporowski, P. Synthesis and Characterization of Ring Polybutadienes. *J. Polym. Sci., Part B: Polym. Phys.* **1988**, *26*, 1251−1259.
(54) Rique-Lurbet, L.; Schappacher, M.; Deffieux, A. A New Strategy for the Synthesis of Cyclic Polystyrenes: Principle and Application. *Macromolecules* **1994**, *27*, 6318−6324.
(55) Wood, B.; Hodge, P.; Semlyen, J. Cyclic Polyesters: 1. Preparation by A New Synthetic Method, Using Polymer-Supported Reagents. *Polymer* **1993**, *34*, 3052−3058.
(56) Hernandez, H. L.; Kang, S.-K.; Lee, O. P.; Hwang, S.-W.; Kaitz, J. A.; Inci, B.; Park, C. W.; Chung, S.; Sottos, N. R.; Moore, J. S.; Rogers, J. A.; White, S. R. Triggered Transience of Metastable Poly(phthalaldehyde) for Transient Electronics. *Adv. Mater.* **2014**, *26*, 7637−7642.
(57) Feinberg, E. C.; Davydovich, O.; Lloyd, E. M.; Ivanoff, D. G.; Shiang, B.; Sottos, N. R.; Moore, J. S. Triggered Transience of Plastic Materials by a Single Electron Transfer Mechanism. *ACS Central Science* **2020**, *6*, 266−273.
(58) Lloyd, E. M.; Lopez Hernandez, H.; Feinberg, A. M.; Yourdkhani, M.; Zen, E. K.; Mejia, E. B.; Sottos, N. R.; Moore, J. S.; White, S. R. Fully Recyclable Metastable Polymers and Composites. *Chem. Mater.* **2019**, *31*, 398−406.
(59) Feinberg, E. C.; Hernandez, H. L.; Plantz, C. L.; Mejia, E. B.; Sottos, N. R.; White, S. R.; Moore, J. S. Cyclic Poly(phthalaldehyde): Thermoforming a Bulk Transient Material. *ACS Macro Lett.* **2018**, *7*, 47−52.
(60) Kremer, K.; Grest, G. S. Dynamics of entangled linear polymer melts: A molecular-dynamics simulation. *J. Chem. Phys.* **1990**, *92*, 5057.
(61) Moreira, L. A.; Zhang, G.; Müller, F.; Stuehn, T.; Kremer, K. Direct equilibration and characterization of polymer melts for computer simulations. *Macromol. Theory Simul.* **2015**, *24*, 419−431.
(62) Kaitz, J. A.; Moore, J. S. Copolymerization of o-Phthalaldehyde and Ethyl Glyoxylate: Cyclic Macromolecules with Alternating Sequence and Tunable Thermal Properties. *Macromolecules* **2014**, *47*, 5509−5513.
(63) Dietz, J. D.; Kroger, M.; Hoy, R. S. Validation and Refinement of Unified Analytic Model for Flexible and Semiflexible Polymer Melt Entanglement. *Macromolecules* **2022**, *55*, 3613−3626.

https://doi.org/10.1021/acspolymersau.2c00069
ACS Polym. Au 2023, 3, 307−317